



The single-crystal diamond trap (SCDT): a new method to determine the composition of high-P–T fluids

Sumith Abeykoon¹ · Andreas Audétat¹

Received: 16 September 2021 / Accepted: 21 December 2021 / Published online: 1 February 2022
© The Author(s) 2022

Abstract

In view of recently reported discrepancies in mineral solubility results obtained with the classical diamond trap method, an alternative approach to quantify the composition of high P–T fluids was developed. In this approach the high P–T fluids are trapped in laser-drilled holes within single-crystal diamond plates and subsequently analyzed by LA–ICP–MS using the same pit size as the one that was used to drill the holes, which allows more rigorous testing of the data reproducibility than in the case of the classical diamond trap, where the fluid resides in a large, open network. To reduce the spikiness of the LA–ICP–MS signals and minimize element fractionation, the aqueous solution within the holes was allowed to evaporate, and the solid residue was melted to a glass. Because this results in the partial loss of the internal standard elements that are usually used for quantifying the LA–ICP–MS signals we developed a new quantification procedure that works without any internal standard in the fluid but instead uses the carbon signal produced by the epoxy that was filled into the holes after melting the precipitates. The new method was first tested on holes filled with epoxy resins doped with known amounts of chemicals, then on holes filled with known amounts of minerals that were subsequently melted, and finally on real high P–T mineral solubility experiments at 1.0 GPa and 700–900 °C in the quartz–H₂O and olivine–enstatite–H₂O systems, for which reliable reference data exist. In all 15 experiments the measured concentrations agree within 1–21% (avg. 13%) with the reference values. In contrast, four mineral solubility experiments that were performed at identical conditions with the classical diamond trap method returned concentrations that deviated by 7–56% (avg. 28%) from the reference value. Furthermore, a strong fractionation effect that has been observed during the ablation of albite + H₂O in a classical diamond trap is efficiently prevented in our single-crystal diamond trap (SCDT) approach. On the downside, we observe significant mobility of alkalis during the melting step in our approach.

Keywords High P–T fluids · Mineral solubility · High P–T experiments · Single crystal diamond trap · LA–ICP–MS · Piston cylinder experiments

Introduction

Various experimental techniques have been used to study the composition of aqueous fluids at ≥ 1 GPa and ≥ 500 °C, including: (i) measuring the weight of single crystals before and after the experiment (e.g., quartz solubility in H₂O; Manning 1994), (ii) constraining the fluid composition via phase relations (e.g., enstatite–forsterite–H₂O system;

Zhang and Frantz 2000), (iii) in-situ observation of dissolving minerals in the hydrothermal diamond anvil cell (e.g., rutile solubility in water; Audétat and Keppler 2005), (iv) trapping fluids in the form of synthetic fluid inclusions and subsequently analyzing them by laser ablation–inductively coupled plasma–mass spectrometry (LA–ICP–MS), which allows only elements that are not abundant in the host mineral to be quantified (e.g., Spandler et al. 2007), (v) in-situ synchrotron–radiation XRF in the hydrothermal diamond anvil cell (e.g., Schmidt et al. 2007), and (vi) the diamond trap method (e.g., Kessel et al. 2004). Of those, the diamond trap method (in the following called "classical diamond trap method") is the most versatile method, because it can be applied in compositionally complex systems, has virtually no limitation with respect to accessible P–T

Communicated by Othmar Müntener.

✉ Sumith Abeykoon
sumith.abeykoon@uni-bayreuth.de

¹ Bayerisches Geoinstitut, University of Bayreuth, 95440 Bayreuth, Germany

conditions, and has also very little limitation with respect to the type and concentration of measurable elements. The diamond trap method was originally developed by Ryabchikov et al. (1989) and was subsequently modified and improved by Kushiro and Hirose (1992), Baker and Stolper (1994), Stalder et al. (2001) and Kessel et al. (2004). This method employs a layer of diamond powder in the experimental capsule, into which fluids/melts infiltrate during the experiment and precipitate dissolved solids during quenching. The diamond layer can subsequently be analyzed by bulk techniques, or—more commonly—by means of in situ LA–ICP–MS analysis. The latter approach has been substantially improved by introducing the “freezing technique” (Kessel et al. 2004), in which the sample capsule is kept frozen during the opening and the subsequent analysis by LA–ICP–MS. This approach avoids spatial fractionation of elements that remain dissolved in the fluid after quenching, such as Cs that is commonly used as internal standard for LA–ICP–MS signal quantification.

A basic assumption behind the diamond trap experiments is that everything analyzed within the diamond trap was dissolved in the fluid at the time of quenching and was in equilibrium with the solid assemblage/mineral. However, this assumption may not always be valid. For example, if the solid starting material is added in the form of a silicate glass, then the aqueous solution will likely get supersaturated during heating and precipitate crystalline phases that may remain in the system during the whole experiment. This phenomenon was documented by in-situ observation of the dissolution of a piece of andesitic glass in water during heating in a diamond anvil cell (Kepler 2017). Minerals that precipitate within the diamond trap during this process will be misinterpreted as dissolved fluid components. Minerals can also form within the diamond trap in response to temperature gradients if the temperature of the diamond trap is lower than that of the surrounding material. High field strength elements (HFSE; Nb, Ta, Zr, Hf, Ti) oxides such as rutile and zircon appear to be particularly sensitive to this effect (Tropper and Manning 2005; Bernini et al. 2013; Rustioni et al. 2021).

Commonly, the LA–ICP–MS signal obtained during slow movement of a laser beam of 50–80 μm size over a frozen diamond trap is relatively constant for some elements, but highly variable for some other elements, such as high field strength elements, for example. The frequency of the signal peaks of the latter elements suggests that local accumulations occur at the scale of 100–200 μm , which is relatively large compared to the grain size of the diamond trap (15–25 μm). This observation raises the question whether these local accumulations represent de-localized solute precipitates that formed during the quench, or whether they reflect material that precipitated already during the run and thus should not be included in the signal interval. Another

potential problem of the classical diamond trap method is elemental fractionation during LA–ICP–MS analysis. Rustioni et al. (2021) analyzed a frozen diamond trap that contained small albite grains and H_2O (and was pressurized, but was never heated) and obtained $\text{SiO}_2/\text{Al}_2\text{O}_3$ ratios that were about twice as high as the theoretical value of albite. In contrast, analyses on a larger piece of the same albite starting material that was analyzed on the same day with the same laser settings returned the correct $\text{SiO}_2/\text{Al}_2\text{O}_3$ ratio. This suggests that in certain mineral–fluid systems severe element fractionation may occur during LA–ICP–MS analysis.

We are aware of only three studies that performed accuracy tests on the diamond trap technique. Aerts et al. (2010) report an accuracy of 3% and a precision of 5% based on a single quartz solubility experiment in H_2O performed at 0.88 GPa and 700 $^\circ\text{C}$, using the solubility data of Manning (1994) as reference. Tiraboschi et al. (2018) report an accuracy of 5% for a single forsterite + enstatite solubility experiment in H_2O conducted at 1.0 GPa and 800 $^\circ\text{C}$, using the solubility data of Newton and Manning (2002) as reference. In contrast, in a more extensive test series based on the solubilities of quartz, forsterite + enstatite, corundum, rutile in H_2O , and supercritical H_2O –albite fluids at 700–800 $^\circ\text{C}$ and 1.0–2.0 GPa, Rustioni et al. (2021) found deviations from reference values ranging from 3% to more than a factor of two, even among identical experiments. The reason for the large discrepancies in some experiments is not clear, but the data suggest that the accuracy of the method can vary dramatically from experiment to experiment, and potentially also from laboratory to laboratory, if, e.g., the temperature distribution or pressure correction in piston cylinder experiments varies. Therefore, it is important to test alternative approaches that may lead to more reproducible results.

Here we present a new method that aims at minimizing the potential problem of mineral precipitation within the diamond trap during the experiment by trapping the high P–T fluid in pre-drilled holes in single diamond crystals, which allows more rigorous testing of the reproducibility of the results than analyzing small parts of the open pore network in a classical diamond trap. Furthermore, with the new method we try to reduce elemental fractionation effects arising from the ablation of spatially unconfined liquid + solid mixtures by letting the liquid to evaporate from the pre-drilled holes and then melting the residue to a glass.

Methods

For our single-crystal diamond trap (SCDT) method we used polished, synthetic diamond plates of about 2.5 mm side length and 0.8–1.0 mm height purchased from Chenguang Machinery & Electric Equipment Co. Ltd., China (~ 10 € per piece). Two such diamond plates were used in each

experiment. Into one of them we drilled 9–16 holes (80 μm diameter; 50–70 μm depth) using a 193 nm ArF Excimer laser that provides a fluence of $\sim 25 \text{ J/cm}^2$ at the sample surface (Fig. 1a). The two diamond plates were then placed on top of each other such that the holes that were drilled into one of the plates were covered by the other plate, and the whole stack was then loaded into a small Pt capsule of 3.5 mm O.D., 3.2 mm I.D. and 5.4 mm length. The Pt capsule was then welded shut, placed into a cold-seal pressure vessel filled with H_2O , and then pressurized to 0.15–0.20 GPa, such that the Pt capsule shrunk tightly around the diamond plates (Fig. 1b). This step is necessary to keep the diamonds tightly together during the subsequent high P–T experiment. After removing the capsule from the vessel it was dried, and then one end of the capsule was cut off with a razor blade to render the diamonds accessible to the fluid. This small, diamond-containing Pt capsule was then loaded together with H_2O and crushed minerals (63–160 μm fraction) into a larger Pt capsule of 5.0 mm O.D., 4.6 mm I.D. and 10 mm length that was sealed using the method described in Audéat and Bali (2010) (Fig. 1b, c). In a few classical diamond trap experiments that were conducted for comparison purpose, the same mineral starting materials were loaded together with a central layer of diamond powder (1:1 ratio of 10–20 μm and 40–60 μm grain size) and aqueous solution containing 200 $\mu\text{g/g}$ of Cs and Rb into

Pt capsules of the same size. The fluid was added to these capsules in several steps following the approach of Rustioni et al. (2021). Finished capsules were checked for leaks by measuring their weights before and after placing them for 2–3 h in a drying oven at 150 $^\circ\text{C}$.

Piston cylinder experiments

High-pressure and high-temperature experiments were conducted in an end-loaded piston cylinder apparatus using $\frac{1}{2}$ inch NaCl–MgO assemblies with a stepped graphite furnace. A constant friction correction of 0.12 GPa was applied based on calibrations involving the quartz–coesite transition at 790 $^\circ\text{C}$ and 2.93 GPa and the densities of synthetic fluid inclusions trapped at 800 $^\circ\text{C}$ and 0.37–9.58 GPa in quartz and corundum single crystals. Temperatures were measured using type S (Pt/Pt–Rh) thermocouples. After pressurization close to the target value, the sample was heated at a rate of 100 $^\circ\text{C}/\text{min}$ to the target temperature. In a final step, pressure was raised to the target value (i.e., hot piston in). Run durations varied depending on the studied system (Table 1), and the experiments were quenched by switching off the electrical power, which resulted in quenching to below 200 $^\circ\text{C}$ within 4–6 s. Once the sample had cooled to room temperature, the remaining pressure was released within 15–30 min. The recovered capsules were checked

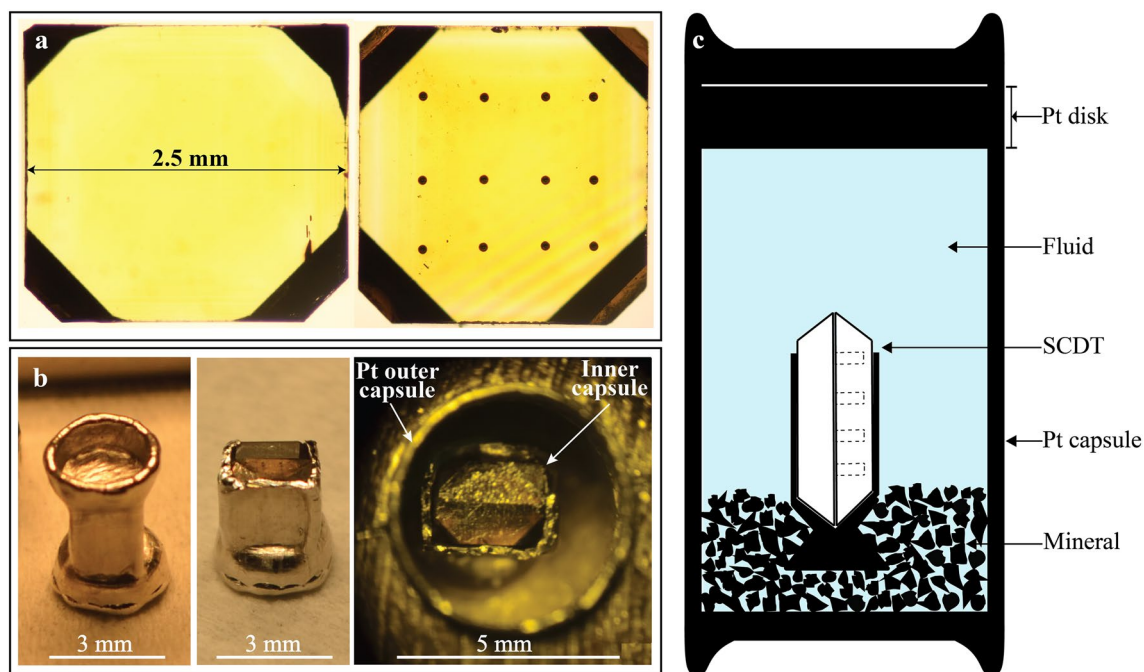


Fig. 1 **a** Photomicrographs of an undrilled (left) and a drilled (right) diamond plate. The holes measure $\sim 80 \mu\text{m}$ in diameter and are ~ 50 – $70 \mu\text{m}$ deep; **b** sealed and shrunk inner capsule (left); one-side cut-open inner capsule (middle); and an inner capsule sitting

inside a platinum outer capsule before filling with fluid; **c** a schematic drawing of the capsule setup, showing the cut-open inner capsule sitting on a bead of crushed minerals. The Pt disk was used to seal the fully fluid-filled Pt capsule of 5.0 mm diameter and 10.0 mm height

Table 1 Summary of experiments and obtained results

Experiment	P (GPa)	T (°C)	Duration (h)	Average $\text{Li}_2\text{B}_4\text{O}_7$ (wt. %)	Reference value (wt. %)	Reference	Density of original solvent (g/cm^3)	Reference value if solvent was H_2O with $1.0 \text{ g}/\text{cm}^3$ (wt. %)	Result with 100 wt. % C as internal standard (wt. %)	Density of precipitate (g/cm^3)	% less volume of epoxy	Corrected result 1st iteration (wt. %)	Corrected result 3rd iteration (wt. %)	% deviation
BaCO_3 in epoxy ^a				0	0.35	Weigh-in	1.15	0.40	0.4 ± 0.1	4.3	0.1	0.40	0.40 ± 0.05	-1
Al_2O_3 in epoxy ^a				0	0.47	"	1.15	0.54	0.4 ± 0.1	4.0	0.2	0.44	0.44 ± 0.04	-19
Al_2O_3 in epoxy ^a				0	5.30	"	1.15	6.05	5.0 ± 0.4	4.0	1.7	4.92	4.92 ± 0.33	-19
TiO_2 in epoxy ^a				0	2.10	"	1.15	2.41	2.2 ± 0.3	4.0	0.7	2.22	2.22 ± 0.28	-8
TiO_2 in epoxy ^a				0	0.32	"	1.15	0.37	0.4 ± 0.1	4.0	0.1	0.40	0.40 ± 0.09	9
TiO_2 in epoxy ^a				0	0.48	"	1.15	0.55	0.6 ± 0.1	4.0	0.2	0.60	0.60 ± 0.12	9
CaF_2 in epoxy ^a				0	0.52	"	1.15	0.60	0.6 ± 0.2	3.2	0.3	0.62	0.62 ± 0.16	3
Epidote in CrystalBond ^b				5.2	17.0	"	1.31	21.18	23.1 ± 5.3	2.6	14.6	19.7	20.1 ± 5.3	-5
Garnet in CrystalBond ^b				2.3	18.5	"	1.31	22.92	21.0 ± 2.1	4.1	8.0	19.3	19.4 ± 2.1	-15
Tourmaline in CrystalBond ^b				3.9	17.0	"	1.31	21.16	19.9 ± 2.3	3.2	10.4	17.8	18.0 ± 2.3	-15
Epidote in CrystalBond ^b				6.0	17.0	"	1.31	21.18	20.4 ± 2.5	2.6	14.1	15.6	17.9 ± 1.7	-16
SCDT—Quartz solubility in water—SA24	1.0	800	3	0	7.0	Manning (1994)	0.89	6.3	7.0 ± 1.3	2.2	4.2	6.7	6.7 ± 1.3	8
SCDT—Quartz solubility in water—SA39	1.0	900	2	5.0	12.6	"	0.85	10.8	13.4 ± 1.9	2.2	10.9	11.9	12.0 ± 1.6	11
SCDT—Forsterite + Enstatite solubility in water—SA31	1.0	800	5	0.7	1.8	Newton and Manning (2002)	0.89	1.6	2.0 ± 0.2	2.2	1.6	1.9	1.9 ± 0.2	21
SCDT—Forsterite + Enstatite solubility in water—SA36	1.0	900	4	15.9	3.1	"	0.85	2.6	2.6 ± 0.8	2.2	8.9	2.3	2.3 ± 0.7	-11
DT—Quartz solubility in water—SA40	1.0	900	5	0	12.6	Manning (1994)	-	-	-	-	-	-	5.5 ± 0.7	-56
DT—Quartz solubility in water—SA41	1.0	800	7	0	7.0	"	-	-	-	-	-	-	5.6 ± 0.5	-20

Table 1 (continued)

Experiment	P (GPa)	T (°C)	Duration (h)	Average Li ₂ B ₄ O ₇ (wt. %)	Reference value (wt. %)	Reference	Density of original solvent (g/cm ³)	Reference value if solvent was H ₂ O with 1.0 g/cm ³ (wt. %)	Result with 100 wt. % C as internal standard (wt. %)	Density of precipitate (g/cm ³)	% less volume of epoxy	Corrected result 1st iteration (wt. %)	Corrected result 3rd iteration (wt. %)	% deviation
DT—Forsterite + Enstatite solubility in water—SA42	1.0	900	8	0	3.1	Newton and Manning (2002)	—	—	—	—	—	—	3.3 ± 0.7	7
DT—Forsterite + Enstatite solubility in water—SA43	1.0	800	10	0	1.8	"	—	—	—	—	—	—	1.3 ± 0.2	-31
SCDT—Eclogite + H ₂ O	2.8	700	15	0	-	-	—	—	—	—	—	—	—	—

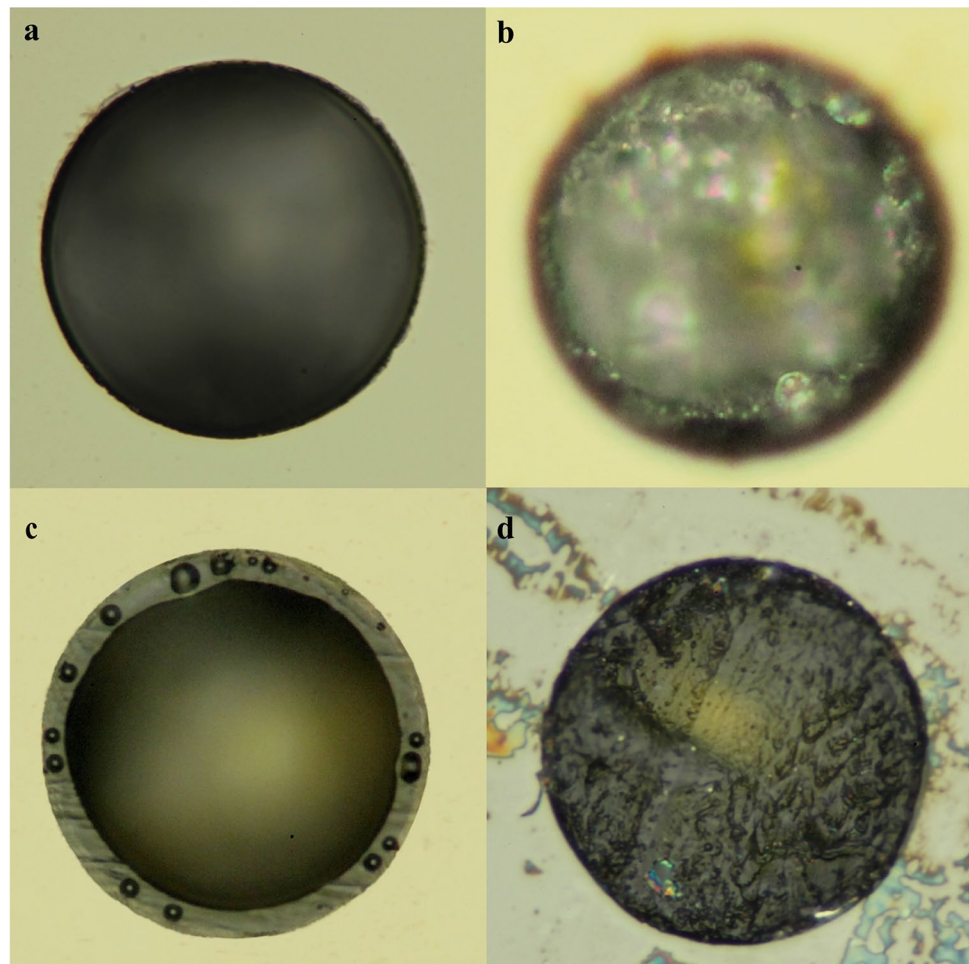
A fictive carbon content of 15 wt. % in the calcite was used for all quantifications

DT classical diamond trap experiments, SCDT single-crystal diamond trap experiments

^aCarefully weighed amounts of fine-grained chemicals were mixed into epoxy and filled into the holes

^bCarefully weighed amounts of pigments were mixed into molten Crystalbond 509. After the mixture was filled into the holes, the Crystalbond was dissolved away in a 2:1 acetone:ethanol mixture

Fig. 2 Photomicrographs of laser-drilled holes in the diamond plates: **a** empty hole before the experiment; **b** after a high P–T quartz solubility experiment, containing precipitated SiO_2 ; **c** after adding $\text{Li}_2\text{O}_4\text{O}_7$ powder and melting at $1000\text{ }^\circ\text{C}$; **d** after filling with epoxy resin, ready to be analyzed with LA–ICP–MS. The diameter of each hole is $80\text{ }\mu\text{m}$. Images **a** and **d** were taken in reflected light; images **b** and **c** in transmitted light



for leaks by visual observation under the binocular and by checking their weights in intervals of several minutes. About one out of six capsules leaked during the experiment. Intact capsules were immediately opened and prepared in the case of the SCDT experiments, whereas in the case of the classical diamond trap experiments they were kept in a freezer at $-20\text{ }^\circ\text{C}$ until the day of the LA–ICP–MS analysis.

Capsule opening and sample preparation

SCDT capsules were cut open at room temperatures using a razor blade. Once opened, part of the liquid residing in the capsule was sucked up with a pipette. The inner capsule was then removed, and the diamond stack was recovered by cutting off some Pt wrapped around them, while the two diamonds remained contacting each other. Special care was taken to keep the diamonds wetted by liquid at all times, including the stage at which the upper diamond was slid off the lower, drilled diamond, as otherwise part of the liquid within the holes is dragged out by surface tension forces during the separation of the diamonds. Permanent wetting was achieved by adding liquid from the pipette. After separating

the diamonds, excess liquid on the lower, drilled diamond plate was quickly scratched off with a clean razor blade, and the holes were allowed to dry. In some cases, the surface was once more cleaned with the razor blade after drying. Attempts to directly fill the holes with epoxy and subsequently analyze them by LA–ICP–MS were not successful, because (i) the precipitates within the holes are commonly loose and ablate very fast, which leads to very spiky signals and (ii) because elements, such as Rb and Cs, which we wanted to use as internal standard, dissolved into the epoxy. As described further below, we thus completely refrained from using an internal standard and quantified the analyses based on the carbon signal of the epoxy filling instead.

To solve the problem with the spiky signals we developed a way to melt the precipitates within the holes and to quench them to a glass without losing too many elements through vaporization. For this purpose, a high-purity, MnO-containing $\text{Li}_2\text{B}_4\text{O}_7$ glass was prepared. Addition of MnO was necessary, because pure $\text{Li}_2\text{B}_4\text{O}_7$ glass is difficult to ablate with the laser. One gram of $\text{Li}_2\text{B}_4\text{O}_7$ (Alfa Aesar, 99.998% purity) was thus mixed with 2 wt. % MnO (Alfa Aesar, 99.99% purity) and melted at $1200\text{ }^\circ\text{C}$ for 12 min in a crimped Pt

capsule. The capsule was then quenched in distilled water and the recovered glass was finely ground in an agate mortar. To add small amounts of this glass to each hole in the SCDT without losing solid precipitates, the fine glass powder was mixed into a ~2:1 acetone–ethanol solution. One drop of this suspension was then placed onto the drilled diamond plate and allowed to dry, resulting in a fine layer of precipitated glass powder evenly spread across the entire surface. Glass powder that precipitated between the holes was then cleaned away using a razor blade. Subsequently, the diamond was covered with a small piece of gold foil (0.2 mm thickness) that was held in place and slightly pushed down with the help of two SiO₂ glass cylinders that fit neatly into a sintered Al₂O₃ tube. The whole setup was then heated for 10 min at 1000 °C inside an 1 atm box furnace. As a result, the precipitates within the holes in the diamond melted and formed a thin glass layer (Fig. 2c). Finally, the holes were filled with epoxy resin (EPOFIX resin mixed with hardener from Struers GmbH, Germany; making sure that no air bubbles were trapped), and excess epoxy was cut away using a razor blade before the epoxy reached full hardness (Fig. 2d).

Preparation of test samples

To calibrate the new quantification approach based on the carbon signal of the epoxy and to test the analytical accuracy of the SCDT method we prepared test samples with known amounts of chemicals or minerals that were placed into the drilled holes in the diamonds. For this purpose, fine-grained Al₂O₃ (< 3 μm), TiO₂ (< 1 μm), BaCO₃ (< 5 μm) and CaF₂ (< 2 μm) chemicals were carefully mixed into epoxy resin in weight proportions of 0.32–5.3 wt. % and filled into the holes. Excess epoxy was cut away using a razor blade. The LA–ICP–MS data were used to calibrate the standardless quantification via the carbon signal (see below). To test the validity of the entire experimental approach including the partial melting step with the added Li₂B₄O₇ it was necessary to add known amounts of solids into the holes without simultaneously adding epoxy. This was achieved by mixing relatively coarse-grained garnet (~ 5 μm), epidote (~ 5 μm) and tourmaline (~ 5 μm) pigments (Enogu mineral pigments series from Kremer Pigments, Aichstetten, Germany) into molten Crystalbond 509, which, after filling the mixture into the holes and cutting excess material away with a razor blade, was subsequently dissolved away using a 2:1 acetone–ethanol solution. The holes were then doped with MnO-bearing Li₂B₄O₇ as described above and melted at 1000° C. Finally, the holes were filled with epoxy, and LA–ICP–MS analysis were performed after the epoxy had hardened overnight. The purity of the MnO-doped Li₂B₄O₇ and the epoxy was checked by LA–ICP–MS analyses. The MnO-doped Li₂B₄O₇ contains 0.37 ± 0.03 wt. % SiO₂ (probably from grinding and mixing the two components in an

agate mortar) but otherwise is very pure (supplementary Table S1), and also the epoxy is very pure (supplementary Table S2). The concentrations and detection limits listed in supplementary Table S1 are representative of the detection limits that can be reached in the analyses of real experimental run products (i.e., less than a few μg/g for most trace elements). The small amount of SiO₂ present in the lithium tetraborate does not significantly affect the calculated solute contents, because even at an extraordinarily high Li₂B₄O₇: solute SiO₂ weight ratio of five it causes only a $(5/6 * 0.0037) / (1/6 * 1.0) = 1.85\%$ increase in the calculated SiO₂ content of a SiO₂-dominated fluid.

LA–ICP–MS analyses

Initially we performed the experiments with Rb- and Cs-doped solutions, with the aim to use these elements as internal standard for quantifying the LA–ICP–MS analyses. A test experiment performed at ambient conditions by filling the holes with a 5 wt. % Na₂SiO₃ solution doped with 100 μg/g each of Rb and Cs, returned reproducible and accurate results (4.9 ± 0.1% relative) for all elements. However, subsequent high P–T experiments performed on model systems (solubility of quartz or enstatite + olivine in H₂O, and supercritical H₂O–albite fluids) with Rb- and Cs-doped aqueous solutions were plagued by poor reproducibility and in average either too high or too low values, which seemed to be at least partly due to problems with the internal standard. Opening the capsules in frozen state and then allowing the ice within the laser holes to melt and slowly dry out in a controlled fashion did not solve the problem. Rather, tests with simple NaCl–KCl–Rb–Cs–Ba–B–Pb solutions (element concentrations ranging from 1 wt.% to 200 μg/g) revealed that freezing amplified the problem, probably because a part of the solution did not freeze and thus remained mobile at the temperature of -20 to -30 °C prevailing in the freezing chamber. Another big problem was the very short, spiky nature of the LA–ICP–MS signals.

To overcome these issues, we started to fill the holes with epoxy resin after they dried out. This increased the length of the LA–ICP–MS signals, but it did not solve the problems with the spiky nature of the signals and the internal standard. During these tests it was observed that the ablation of epoxy produces a much higher carbon signal than the ablation of diamond (because the ablation rate in epoxy is much faster), which opens up the possibility to use the epoxy filling instead of a fluid component as the internal standard. However, such an approach is fundamentally different from the normal way of using internal standards: the carbon signal of the epoxy can only be used to quantify the weight of the precipitates relative to the weight of the epoxy that fills out the rest of the hole. To transform this value into the amount of solids dissolved within the fluid, it is

thus necessary to make corrections for the density difference between epoxy and fluid, and for the space occupied by the precipitates + $\text{Li}_2\text{B}_4\text{O}_7$ (see below).

In the case of the few comparison runs performed with the classical diamond trap technique the capsules were first dropped into liquid nitrogen before opening them longitudinally with a sturdy razor blade in an opening device that had a temperature of ca. -30 to -60 °C. One half of the frozen capsule was then quickly transferred to an LA-ICP-MS sample chamber that was cooled to ca. -30 °C (according to tests with H_2O -ethanol solutions) by means of a Peltier cooling element to keep the sample frozen also during the measurement (Kessel et al. 2004; Aerts et al. 2010). In those experiments, the Cs concentration in the starting solution was used as the internal standard for calculating absolute element concentrations, accounting for the lowering of the original concentration due to the dissolution of solids.

The LA-ICP-MS analyses were performed with a 193 nm ArF Excimer laser (GeolasPro system; Coherent; USA) attached to a quadrupole mass spectrometer (Elan DRC-e; Perkin Elmer; Canada). To increase the length of the LA-ICP-MS signals the epoxy-filled holes were ablated with a lower repetition rate (5 Hz) and a lower energy (40–65 mJ) than the external standards (10 Hz, 90–110 mJ). For ablating the epoxy-filled holes in the diamonds we used the same laser diameter (80 μm) as the one that had previously been used to drill the holes. The sample chamber was flushed with He gas at a rate of 0.4 l/min, to which 5 ml/min H_2 was added on the way to the ICP-MS. The latter was tuned to a ThO production rate of 0.5–1.5% and a production rate of doubly-charged ^{42}Ca ions of 0.15–0.30 based on measurements on NIST SRM 610 glass. Analyzed isotopes include ^7Li , ^{11}B , ^{12}C , ^{23}Na , ^{25}Mg , ^{27}Al , ^{29}Si , ^{30}Si , ^{31}P , ^{35}Cl , ^{39}K , ^{43}Ca , ^{49}Ti , ^{53}Cr , ^{55}Mn , ^{57}Fe , ^{59}Co , ^{62}Ni , ^{65}Cu , ^{66}Zn , ^{85}Rb , ^{88}Sr , ^{89}Y , ^{90}Zr , ^{133}Cs , ^{137}Ba , ^{139}La , ^{140}Ce , ^{157}Gd , ^{175}Lu , ^{208}Pb , ^{232}Th , and ^{238}U , using dwell times of 10–20 ms. For external standardization we used either NIST SRM 610 (Jochum et al. 2011) or USGS GSE-1G as reference material (for the latter we used the GeoReM preferred values of 7/2018), plus a natural calcite crystal from Iceland as a calibrant for the carbon signal. Signal integration, spike removal, and numerical calculations were done using two in-house Excel spreadsheets. The quantification spreadsheet allows two external standards to be used simultaneously. As internal standard we used in a first stage the carbon signal of the ablated epoxy. Attempts to dope the epoxy with trace elements and use one of these elements as internal standard failed, because we did not manage to manufacture epoxy in which the trace elements are homogeneously distributed at the micrometer scale. Due to the different ablation behavior of epoxy relative to minerals, it is not possible to take the actual carbon content of the epoxy as internal standard. Instead, we used a fictive carbon concentration of 100 wt. %

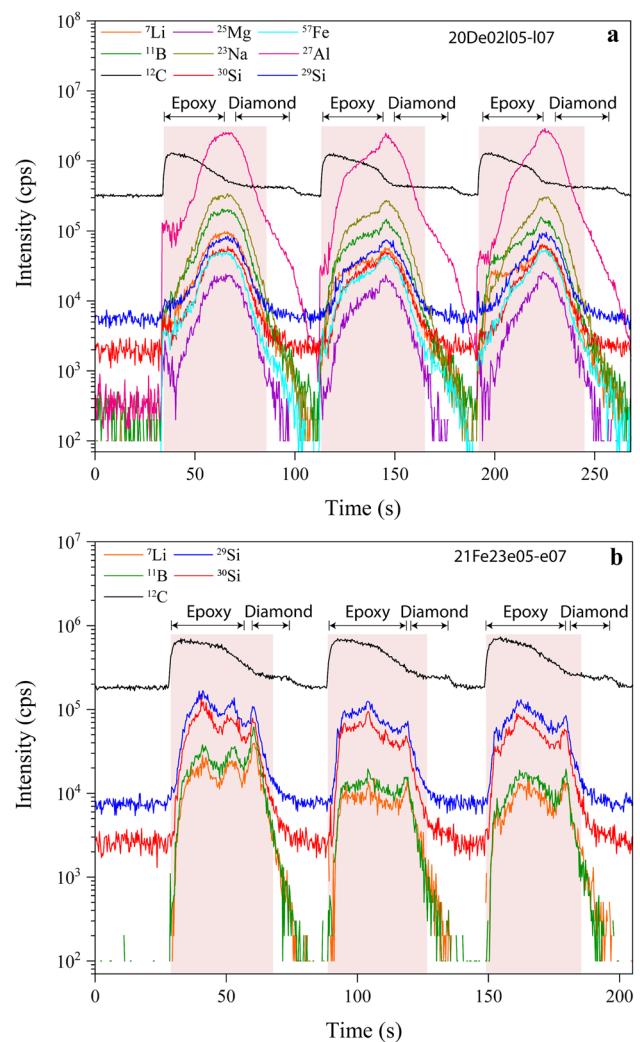


Fig. 3 LA-ICP-MS signals of SCDT analyses; **a** signal of three different holes containing 18.0 ± 2.3 wt. % of tourmaline pigment; **b** three analyzed holes of the quartz+water experiment at 1.0 GPa, 900 °C containing in average 12.0 ± 1.6 wt. % of SiO_2 . The shaded areas show the signal integration intervals of each hole

and changed via the "goal seek" analysis tool in Excel the carbon content of the calcite until the best average result was obtained for the experiments in which the holes were filled with known amounts of Al_2O_3 , TiO_2 , BaCO_3 and CaF_2 using very fine-grained mixtures in epoxy. The same could have been done using the correct carbon concentration for calcite and finding via the goal seek function a fictive carbon concentration in the epoxy, but for the calculations the former approach is more practical. In either case, the fictive carbon value that is found via the goal seek function likely depends on ICP-MS instrument and laser ablation settings and thus has to be calibrated for each laboratory individually based on test samples as described above. However, it does not seem to be necessary to re-calibrate the fictive carbon in each analytical session, as test samples analyzed on

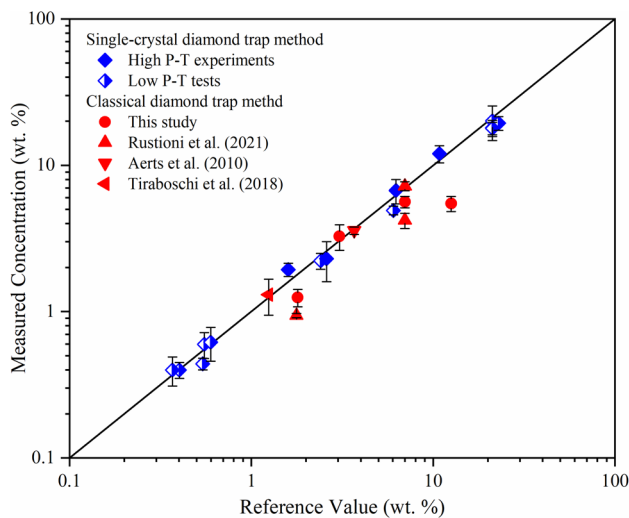


Fig. 4 Comparison between measured weight percentages and reference values for tests and experiments conducted with the SCDT method (blue diamonds) vs. experiments conducted with silicate materials using the classical diamond trap method (red circles and triangles). The black line represents the 1:1 line, i.e., perfect agreement between measured and reference values

15 different measuring days spread over a 5 months period using a constant fictive carbon value for the calcite (15 wt. % in our case) returned consistent results.

Another important difference to the normal way of internal standardization is that corrections need to be made to account for the difference in the density of epoxy vs. the density of the medium in which the solutes were dissolved or immersed originally. For example, if, e.g., SiO_2 was originally dissolved in a high P–T H_2O fluid with a density of 0.89 g/cm^3 , and the holes are then filled with pure epoxy with a density of 1.15 g/cm^3 , then a correction of $(1.15/0.89) - 1.0 = +29\%$ has to be applied to the concentration values determined based on epoxy. Because we used calibrants with various densities (epoxy with 1.15 g/cm^3 , Crystalbond 509 with 1.31 g/cm^3 , and aqueous solutions with $0.85\text{--}0.89 \text{ g/cm}^3$) we decided to normalize all concentrations to a solvent density of 1.00 g/cm^3 before determining the fictive carbon concentration of the calcite (Table 1). This means that for any new solubility measurement the results are first obtained for an assumed solvent density of 1.0 g/cm^3 , and then a correction needs to be applied to account for the actual solvent density.

A last issue concerns the difference between the density of the solvent vs. the density of the bulk fluid (i.e., solvent + solute). At solute contents of less than a few weight percent the difference between the two values is negligible, but at higher solute content it becomes significant, such that an additional correction is required. A visual way to deal with this issue is to think in terms of space occupied by the precipitated solutes (plus added $\text{Li}_2\text{B}_4\text{O}_7$) vs. space occupied

by the remaining solvent (now filled with epoxy). If, e.g., one-third of the hole is filled with precipitates (plus added $\text{Li}_2\text{B}_4\text{O}_7$) instead of with epoxy, then the result calculated on the basis of an internal carbon concentration of 100 wt.% will turn out 33% too high. If the density of the epoxy, the weight percentage of the precipitates and the average density of the latter are known, then the amount of overestimation equals to:

$$\% \text{overestimation} = \left[\frac{\text{wt.\%solute}}{\text{density of precipitates}} + \frac{\text{wt.\%added } \text{Li}_2\text{B}_4\text{O}_7}{\text{density of } \text{Li}_2\text{B}_4\text{O}_7} \right] \times \left[\frac{\text{density of epoxy}}{100/\text{density of epoxy}} \right] \times 100$$

However, the weight percentage of solute is what we are actually looking for, hence the correct value can only be found iteratively. In the first step, it is assumed that the entire hole is filled with epoxy, which gives a certain weight percent solute. That value is then used to calculate a corrected weight percent value, which is then used to calculate a further refined value. After three iterations a stable result ($< 1\%$ difference relative to the previous iteration) value is obtained even for high solute contents of 20–30 wt. %. It should be stressed that the magnitude of this final correction procedure is small: for 10 wt. % solute it amounts to $\leq 6\%$ (the exact value depending on the fluid density, and thus on the P–T conditions), i.e., the value of 10 wt. % needs to be correct down to 9.4 wt. % at most. An Excel spreadsheet with the full calculation details of experiment SA31 is provided in the electronic supplementary material.

Results

Representative LA–ICP–MS signals obtained from SCDT experiments are shown in Fig. 3. Figure 3a shows the signals of three holes analyzed from a test experiment performed with 17 wt. % tourmaline pigment, whereas Fig. 3b shows the signals of three holes analyzed from a quartz solubility experiment in water at 1.0 GPa, 900 °C (the reference solubility value for the latter experiment is 12.6 wt. % SiO_2 ; Manning 1994). The net carbon signal obtained from the ablation of epoxy is about 6 times higher than the net signal obtained during the ablation of diamond, hence even if part of the chosen signal interval extends into the diamond domain (Fig. 3a) the bulk of the net carbon signal is still heavily dominated by the epoxy. The reason why the signal of the melted solids within the holes commonly extends beyond the signal of the epoxy is that the glass tends to accumulate at the bottom of the hole.

After calibrating the new method based on holes filled with epoxy that was doped with known amounts of chemicals (Al_2O_3 , TiO_2 , BaCO_3 , CaF_2), the sample melting

procedure with the added MnO-doped $\text{Li}_2\text{B}_4\text{O}_7$ was tested with a series of experiments in which known amounts of mineral pigments (garnet, epidote, tourmaline) were filled into the holes with the help of Crystalbond 509 that was subsequently dissolved away. The expected values (calculated from the weights of pigments mixed into Crystalbond) for the garnet, epidote, tourmaline tests are 22.9, 21.2 and 21.2 wt. %, respectively, and the obtained results agree with these reference values within 5–16%. In addition, the measured compositions of the melted minerals agree well (within 1 wt. % absolute) with those obtained through LA–ICP–MS analysis of densely pressed pellets produced from the same pigment powders, except for the Al_2O_3 content of the tourmaline, which turned out 7 wt. % too high, and the K_2O content of one of the two tests performed with epidote, which was 2 wt. % too high (supplementary Table S3). Whereas the reason for the higher Al_2O_3 content of the melted tourmaline is not clear, gains of K_2O during the melting procedure were relatively common and appear to have been caused by contamination of the furnace or some other parts of the melting assembly (see below).

A more detailed check for potential losses or gains of elements during the melting procedure was performed by loading small amounts of crushed GSE-1G reference glass plus MnO-doped $\text{Li}_2\text{B}_4\text{O}_7$ at a weight ratio of ca. 2:1 into the laser-drilled holes in a diamond, melting them in the usual manner (i.e., at 1000 °C; with the holes covered by an Au foil), and then filling the remaining space of the holes with epoxy before the LA–ICP–MS analysis. The results (supplementary Table S4) reveal that most of the major and minor element concentrations remained unmodified, except for Na_2O and K_2O , which experienced gains of 50% and

130%, respectively (1.8 wt. % Na_2O and 3.4 wt. % K_2O on an absolute basis). The results with respect to changes in trace element concentrations are varied: six out of 19 analyzed trace changed by less than 10%; nine elements decreased by 10–25%; and Cs, Cu, Ag and Cd decreased by 35 to > 147% (supplementary Table S4).

A final test to investigate potential losses or gains of elements during the melting procedure was performed by adding variable amounts of albite powder into the holes (the exact amounts being unknown, but visually estimated to be in the range of 1–20 wt. %) and melting them as described above. The LA–ICP–MS analyses revealed SiO_2 , Na_2O and Al_2O_3 concentrations that agree within 2% with those of the starting material, but about 3.8 wt. % K_2O were gained (supplementary Table S3). Remember that a similar test performed on an albite-doped classical diamond trap returned a $\text{SiO}_2/\text{Al}_2\text{O}_3$ concentration ratio that was wrong by a factor of two (Rustioni et al. 2021), apparently due to element fractionation occurring during the ablation of the diamond + albite + ice/liquid H_2O mixture (Rustioni et al. 2021). The present test thus suggests that the SCDT method greatly helps to reduce fractionation effects occurring during the LA–ICP–MS analysis of classical diamond traps, but alkalis may be significantly gained (or lost) during the melting procedure.

Finally, the experiments were expanded to real solubility measurements at high pressure and temperature in the well-studied H_2O – SiO_2 and H_2O –enstatite–olivine systems, for which reliable reference data exist (Manning 1994; Newton and Manning 2002). A summary of all the previously described tests and the high P , T runs is provided in Table 1 and Fig. 4. With regard to quartz solubility in water we performed two SCDT experiments at 1.0 GPa pressure and 800 °C and 900 °C, respectively, plus two classical diamond trap experiments at the same conditions for comparison. Previous experimental studies returned consistent results within this range of P – T conditions (Anderson and Burnham 1965; Fournier and Potter 1982; Manning 1994), allowing us to use these data as a reference. Our experiments at 800 °C and 900 °C agree with the reference values within +8% and +11%, respectively. The same experiments performed using the classical diamond trap method show 20% deviation at 800 °C and 56% deviation at 900 °C. Aerts et al. (2010) report only -3% deviation for a classical diamond trap experiment performed at 0.88 GPa and 700 °C, whereas Rustioni et al. (2021) performed two experiments (also using the classical approach) at 1.0 GPa and 800 °C and found +3% discrepancy in one of them, and -40% discrepancy in the other. The reason for the large discrepancies in some of these experiments is not clear. If it was due to erroneous temperature reading due to thermal gradients between thermocouple and sample, then these gradients would have to be nearly 100 °C, which seems unlikely (see below). Run duration should not have been the problem either, as our SCDT experiments were run only for 2–3 h and returned already good agreement, whereas our

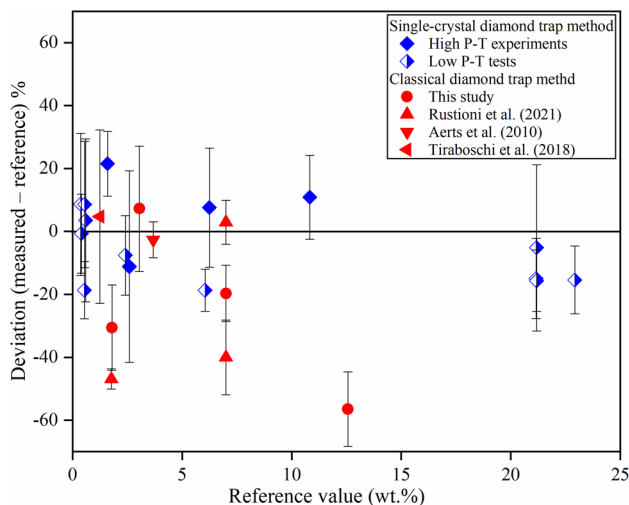


Fig. 5 Relative deviation (in %) of the measured weight percentages from the reference values as a function of the absolute weight percentages. Blue diamonds denote the SCDT method, whereas red circles and triangles denote the classical diamond trap method, Fig. 1

classical diamond trap experiments were run for 5–7 h, and those of Rustioni et al. (2021) for 16–18 h. One potential explanation would be preferential loss of H₂O during the experiment, which would lead to an increase in the Cs concentration in the remaining fluid and thus in an underestimation of the SiO₂ solubility. Another potential explanation is that during the opening of the frozen diamond trap some Cs-rich, residual solution was expelled onto the diamond trap surface.

The solubility of SiO₂ in the forsterite–enstatite–water system was measured at 1.0 GPa and 800 to 900 °C. Our SCDT results agree with the Newton and Manning (2002) data within +21% at 800 °C, and within -11% at 900 °C. In comparison, the results of our classical DT experiments agree with the literature values within -31% at 800 °C, and within +7% at 900 °C. A classical diamond experiment performed by Rustioni et al. (2021) at 1.0 GPa and 800 °C resulted in 47% underestimation of the SiO₂ solubility, whereas Tiraboschi et al. (2018) obtained an agreement within +5% at the same conditions. Again, run time is unlikely to be responsible for the discrepancies, as our SCDT experiments were run for 4–5 h, whereas our classical diamond trap experiments were run for 8–10 h, that of Rustioni et al. (2021) for 20 h, and that of Tiraboschi et al. (2018) for ~48 h. Considering all experiments and test runs, the new SCDT method produced results that deviate maximal 21% from the reference values (average deviation 13%), whereas identical experiments using the classical diamond trap method deviate by up to 56% (average deviation 28%; Fig. 5). The large negative deviations of some classical diamond trap experiments are unlikely to be caused by short run times, because other classical diamond trap experiments of similar duration returned correct results and because the SCDT experiments lasted only half as long. We tried to avoid unnecessarily long experimental run times, because this promotes the dissolution and re-precipitation of minerals in thermal gradients and thus may cause positive deviations from reference values. One advantage of the new SCDT method over the classical diamond trap method is that it allows use of very high fluid/solid ratios. This facilitates the growth of large crystals during the experiments and thus the determination of fluid–mineral partition coefficients of trace elements. For example, we conducted a SCDT experiment with a crushed eclogite as starting material and recovered large crystals of pyroxene, garnet and mica after a run duration of only 15 h (supplementary Figure S1).

Discussion

According to the results presented above the new SCDT method provides more reliable mineral solubility data at high *P–T* conditions than corresponding data obtained

with the classical diamond trap technique in our lab. However, as with any experimental or analytical technique, the results can be affected by a number of sources of uncertainty. In decreasing order of estimated relevance these are: (1) temperature differences between the thermocouple and the diamond trap; (2) loss or addition of material from/to the holes during sample preparation after the experiments; (3) fractionation effects during LA–ICP–MS analysis; (4) gains or losses of alkalis during the melting procedure, (5) wrong assumptions made in the quantification approach (e.g., regarding the density of the precipitates); and (6) day-to-day variations in the sensitivity of the carbon relative to other elements.

Recent experiments to quantify temperature gradients within Pt capsules of piston cylinder experiments revealed that with the standard 1/2" assemblies used at BGI (a talc-pyrex-crushable Al₂O₃ assembly and a MgO–NaCl assembly; the latter being used in the present study) temperature gradients between thermocouple and the center of the Pt capsule can easily reach ±50 °C, depending on how the graphite heater deforms during initial pressurization (Audétat et al. 2020). A temperature offset of ±50 °C at our experimental conditions results in a SiO₂ solubility difference of ±0.5 wt. % in the forsterite–enstatite–H₂O system, and ±1–3 wt. % in the quartz–H₂O system, corresponding to errors of 28% and 14–43%, respectively.

Loss or addition of material from/to the holes during sample preparation can occur due to shaky hands. In addition, excess minerals may form within some holes due to dissolution–reprecipitation in response to temperature gradients, or due to metastability effects during heating (Keppler, 2017). However, in contrast to the classical diamond trap method, these effects can be readily noticed in SCDT experiments by anomalous results obtained from certain holes. Indeed, in five of our fifteen SCDT experiments some holes were strongly anomalous and thus were not considered in the calculation of the average (see the calculations of experiment SA31 in the supplementary material as an example). This is perhaps the biggest advantage of the SCDT method over the classical approach, as each sample volume is clearly defined, whereas in the classical approach it is up to the user how to choose the integration intervals.

Our tests with mineral pigments and albite added to unheated single-crystal diamond traps suggest that fractionation effects during laser ablation are small. In particular, the test with the albite revealed an agreement with the theoretical values within 6%, which is a major improvement compared to a similar test performed by Rustioni et al. (2021) with the classical diamond trap, in which a discrepancy of a factor of two was noticed. The analyses of garnet, epidote, tourmaline albite and silicate glass powders that were filled into the holes in the diamond and

subsequently melted in the presence of lithium tetraborate revealed SiO_2 , Al_2O_3 , MgO , FeO_{tot} and TiO_2 concentrations that generally agree within 1 wt. % with the compositions of the starting materials, except for Na_2O and K_2O , which in some tests were gained in appreciable amounts (supplementary Tables S3 and S4).

The standardless quantification approach requires input of the density of the precipitates within the holes after the experiment, and that of the solvent at run conditions. The former can only be estimated. In our high P–T runs the bulk of dissolved matter was dominated by SiO_2 . For simplicity we thus assumed that the precipitates after the experiment consist of SiO_2 glass, and that the density of SiO_2 dissolved in the fluid was the same as that of SiO_2 glass (although the latter is not perfectly true, e.g., Hunt and Manning 2012). In this case the density of the solvent corresponds to the density of H_2O , which was calculated based on Saul and Wagner (1987). Since the amount of dissolved matter in our high P–T runs was relatively low (≤ 12 wt. %) the calculated concentrations are rather insensitive to the assumptions regarding the density of the precipitates and the density of dissolved matter in the fluid: changing the value by 30% causes the calculated concentration of dissolved matter to change by only 2–3%. Finally, since the standardless quantification is based on the carbon signal, which shows a high background value (Fig. 3), day-to-day or within-day variations in the sensitivity of carbon relative to other elements may represent another source of uncertainty. However, within 15 measuring days spread out over 5 months we did not notice any systematic shift in the fictive carbon value of the calcite that was required to obtain optimal agreement between measured concentration values and the reference values. We thus believe that variations in the sensitivity of carbon do not represent a large source of uncertainty in the SCDT approach, at least if the ICP–MS is used in a similar fashion as in the current study.

Conclusions

Our newly developed SCDT method for studying fluid compositions in high-P and high-T experiments offers the following advantages over the classical diamond trap approach:

- The use of spatially separated holes to retain the high-pressure fluids during quench allows a more reliable testing of the reproducibility of solubility data. Outliers caused by growth of minerals within certain holes during the run, or gain/loss of mineral precipitates during the sample preparation can be readily identified and be excluded from the data set.

- At least in the present study the SCDT method produced better reproducible and more accurate results than the classical diamond trap approach.
- Less element fractionation (i.e., test with albite)
- No freezing stage is necessary to analyze the diamond trap.
- The method can (but does not necessarily have to) be used with very high fluid/solid ratios, which promotes the growth of large crystals that are required to determine fluid–mineral partition coefficients for mineral-incompatible trace elements.

The main disadvantages of the SCDT method are the following:

- Both the sample preparation before the experiments (drilling of diamonds; preparation of inner capsules) and the sample preparation after the experiments (addition of $\text{Li}_2\text{B}_4\text{O}_7$; melting; filling of the residual space with epoxy) is more time consuming and requires clean, careful handling without shaky hands.
- Compared to the classical diamond trap approach also the quantification procedure of the LA–ICP–MS signals is more difficult and time consuming. On the other hand, the fact that no internal standard in the fluid is necessary may prove helpful in experiments in which none of the available elements behaves incompatibly enough to be used as internal standard.
- Alkalies may be gained or lost during the melting step.
- Finally, one needs to purchase single-crystal diamond plates. However, they cost only 10–20 € each, depending where one buys them.

Overall, we believe that the SCDT method is a viable alternative to the classical diamond trap method and provides reliable mineral solubility data in high P–T fluids.

Supplementary Information The online version contains supplementary material available at <https://doi.org/10.1007/s00410-021-01882-6>.

Acknowledgements We would like to thank Raphael Njul and Alexander Rother for help with epoxy and test filling materials preparation, Stefan Übelhack and Sven Linhardt for manufacturing the Peltier element-cooled ablation cell and other devices. Sincere thanks also to Othmar Müntener, Bob Luth and an anonymous reviewer for their thorough reviews, which greatly helped to improve the manuscript. This study was conducted under the “Deep volatile cycles – International Research Training Group” funded by German Research Foundation (Deutsche Forschungsgemeinschaft – DFG, GRK 2156/1).

Funding Open Access funding enabled and organized by Projekt DEAL.

Open Access This article is licensed under a Creative Commons Attribution 4.0 International License, which permits use, sharing, adaptation, distribution and reproduction in any medium or format, as long as you give appropriate credit to the original author(s) and the source, provide a link to the Creative Commons licence, and indicate if changes were made. The images or other third party material in this article are included in the article's Creative Commons licence, unless indicated otherwise in a credit line to the material. If material is not included in the article's Creative Commons licence and your intended use is not permitted by statutory regulation or exceeds the permitted use, you will need to obtain permission directly from the copyright holder. To view a copy of this licence, visit <http://creativecommons.org/licenses/by/4.0/>.

References

- Aerts M, Hack AC, Reusser E, Ulmer P (2010) Assessment of the diamond-trap method for studying high-pressure fluids and melts and an improved freezing stage design for laser ablation ICP-MS analysis. *Am Mineral* 95:1523–1526. <https://doi.org/10.2138/am.2010.3356>
- Anderson GM, Burnham CW (1965) Solubility of quartz in supercritical water. *Am J Sci* 263:494–511
- Audétat A, Bali E (2010) A new technique to seal volatile-rich samples into platinum capsules. *Eur J Mineral* 22:23–27. <https://doi.org/10.1127/0935-1221/2010/0022-1982>
- Audétat A, Keppler H (2005) Solubility of rutile in subduction zone fluids, as determined by experiments in the hydrothermal diamond anvil cell. *Earth Planet Sci Lett* 232:393–402. <https://doi.org/10.1016/j.epsl.2005.01.028>
- Audétat A, Krupp A, Putra R (2020) Mapping the temperature distribution within piston cylinder sample capsules. Annual report Bayerisches Geoinstitut, pp 146–147
- Baker MB, Stolper EM (1994) Determining the composition of high-pressure mantle melts using diamond aggregates. *Geochim Cosmochim Acta* 58:2811–2827. [https://doi.org/10.1016/0016-7037\(94\)90116-3](https://doi.org/10.1016/0016-7037(94)90116-3)
- Bernini D, Audétat A, Dolejš D, Keppler H (2013) Zircon solubility in aqueous fluids at high temperatures and pressures. *Geochim Cosmochim Acta* 119:178–187. <https://doi.org/10.1016/j.gca.2013.05.018>
- Fournier RO, Potter RW (1982) An equation correlating the solubility of quartz in water from 25 482 °C to 900 °C at pressures up to 10,000 bars. *Geochim Cosmochim Acta* 46:1969–1973. [https://doi.org/10.1016/0016-7037\(82\)90135-1](https://doi.org/10.1016/0016-7037(82)90135-1)
- Hunt JD, Manning CE (2012) A thermodynamic model for the system SiO₂-H₂O near the upper critical end point based on quartz solubility experiments at 500–1100 °C and 5–20kbar. *Geochim Cosmochim Acta* 86:196–213. <https://doi.org/10.1016/j.gca.2012.03.006>
- Jochum KP, Weis U, Stoll B et al (2011) Determination of reference values for NIST SRM 610–617 glasses following ISO guidelines. *Geostand Geoanalytical Res* 35:397–429. <https://doi.org/10.1111/j.1751-908X.2011.00120.x>
- Keppler H (2017) Fluids and trace element transport in subduction zones. *Am Mineral* 102:5–20. <https://doi.org/10.2138/am-2017-5716>
- Kessel R, Ulmer P, Pettko T, Schmidt MW, Tompson AB (2004) A novel approach to determine high-pressure high-temperature fluid and melt compositions using diamond-trap experiments. *Am Mineral* 89:1078–1086. <https://doi.org/10.2138/am-2004-0720>
- Kushiro I, Hirose K (1992) Experimental determination of composition of melt formed by equilibrium partial melting of peridotite at high pressures using aggregates of diamond grains. *Proc Jpn Acad* 68:63–68
- Manning CE (1994) The solubility of quartz in H₂O in the lower crust and upper mantle. *Geochim Cosmochim Acta* 58:4831–4839. [https://doi.org/10.1016/0016-7037\(94\)90214-3](https://doi.org/10.1016/0016-7037(94)90214-3)
- Newton RC, Manning CE (2002) Solubility of enstatite + forsterite in H₂O at deep crust/upper mantle conditions: 4 to 15 kbar and 700 to 900°C. *Geochim Cosmochim Acta* 66:4165–4176. [https://doi.org/10.1016/S0016-7037\(02\)00998-5](https://doi.org/10.1016/S0016-7037(02)00998-5)
- Rustioni G, Audétat A, Keppler H (2021) A systematic assessment of the diamond trap method for measuring fluid compositions in high-pressure experiments. *Am Mineral* 106:28–37. <https://doi.org/10.2138/am-2020-7453>
- Ryabchikov I, Orlova G, Kalenchuk GY, Ganeyev II, Udovkina NG, Nosik LP (1989) Reactions of spinel lherzolite with H₂O-CO₂ fluids at 20 kbar and 900 °C. *Geochem Int* 26:56–62
- Saul A, Wagner W (1987) International equation for the saturation properties of ordinary water substance. *J Phys Chem Ref Data* 16:893–901. <https://doi.org/10.1063/1.555787>
- Schmidt K, Rickers K, Bilderback DH, Huang R (2007) In situ synchrotron-radiation XRF study of REE phosphate dissolution in aqueous fluids to 800 °C. *Lithos* 95:87–102. <https://doi.org/10.1016/j.lithos.2006.07.017>
- Spandler C, Mavrogenes J, Hermann J (2007) Experimental constraints on element mobility from subducted sediments using high-P synthetic fluid/melt inclusions. *Chem Geol* 239:228–249. <https://doi.org/10.1016/j.chemgeo.2006.10.005>
- Stalder R, Ulmer P, Thompson AB, Günther D (2001) High pressure fluids in the system MgO-SiO₂-H₂O under upper mantle conditions. *Contrib Mineral Petrol* 140:607–618. <https://doi.org/10.1007/s004100000212>
- Tiraboschi C, Tumiati S, Sverjensky D, Pettko T, Ulmer P, Poli S (2018) Experimental determination of magnesia and silica solubilities in graphite-saturated and redox-buffered high-pressure COH fluids in equilibrium with forsterite+enstatite and magnesite+enstatite. *Contrib Mineral Petrol* 173:1–17. <https://doi.org/10.1007/s00410-017-1427-0>
- Tropper P, Manning CE (2005) Very low solubility of rutile in H₂O at high pressure and temperature, and its implications for Ti mobility in subduction zones. *Am Mineral* 90:502–505. <https://doi.org/10.2138/am.2005.1806>
- Zhang YG, Frantz JD (2000) Enstatite-forsterite-water equilibria at elevated temperatures and pressures. *Am Mineral* 85:918–925. <https://doi.org/10.2138/am-2000-0705>

Publisher's Note Springer Nature remains neutral with regard to jurisdictional claims in published maps and institutional affiliations.